

Calculated electronic structure and magnetic properties of Y-Fe compounds

R. Coehoorn

Philips Research Laboratories, P.O. Box 80 000, NL-5600 JA Eindhoven, The Netherlands

(Received 5 December 1988; revised manuscript received 15 March 1989)

Results of self-consistent *ab initio* band-structure calculations using the augmented-spherical-wave method are presented for the stable intermetallic compounds Y_2Fe_{17} , Y_6Fe_{23} , YFe_3 , and YFe_2 and for the hypothetical compound YFe_5 . The calculated magnetic moments agree well with the experimental data, if a small orbital contribution to the total moment is assumed. The calculated equilibrium volume is systematically 6–7% too small. This is attributed to (i) a failure of the local-spin-density-functional approximation in describing the contribution of the Fe sublattice to the total volume, and (ii) an underestimate of the contribution of the Y sublattice. The calculations explain the anomalously large volume and magnetization of Y_6Fe_{23} , while the calculated magnetic moments on its four inequivalent sites agree well with neutron diffraction data. The volume dependence of the magnetization of each site in the Y-Fe compounds is related to the density of states at the Fermi level by a simple, but quite accurate expression.

I. INTRODUCTION

In the last two decades the Y-Mn, Y-Fe, Y-Co, and Y-Ni binary compounds have been studied extensively, not only because of their own interesting properties, but also because they are prototypes for the interesting class of 4f-rare-earth-3d-transition-metal (RE-TM) compounds.¹ Investigations of the yttrium compounds can reveal the contribution of the 3d sublattice to the magnetic properties of the RE-TM compounds, because the nonmagnetic Y atom is chemically very similar to the trivalent rare-earth atoms. The contribution of the rare-earth atoms to the magnetization and the magnetic anisotropy is relatively well understood on the basis of the atomic-level structure of the trivalent rare-earth atoms, perturbed slightly by the crystal field and by weak exchange interactions with the transition-metal (M) atoms that are mediated by the rare-earth 5d states.² On the other hand, the 3d-transition-metal electrons have a much more itinerant character. Therefore their contribution to the magnetic properties is strongly dependent on the crystal structure and lattice parameters.

Electronic-structure calculations of many Y-M compounds have been performed by Inoue *et al.*³ and Shimizu *et al.*⁴ using the recursion method and by Yamada *et al.*⁵ using also the tight-binding approximation. Both methods are non-self-consistent. They calculated the density of states (DOS), the local magnetic moments, the high-field susceptibility χ_{hf} , and the coefficient γ of the electronic contribution to the low-temperature specific heat. Using the calculations several interesting phenomena were discussed like the thermal spontaneous ferromagnetism in Y_2Ni_7 , the metamagnetism in YCo_2 , and in the off-stoichiometric compound Y_2Ni_{16} , and the (possible) ferromagnetism of the superconducting compound Y_9Co_7 . Often, good agreement between the calculated and experimental physical properties was obtained. However, self-consistent calculations of YCo_2 (Ref. 6)

and YFe_2 (Ref. 7) by Mohn and Schwarz using the augmented-spherical-wave (ASW) method showed that the majority- and minority-spin DOS's are shaped differently due to differences in the yttrium-transition-metal covalent interaction for majority- and minority-spin electrons. These effects were not taken into account in the non-self-consistent calculations mentioned previously. Other important aspects of self-consistent calculations are the possibilities for calculating the equilibrium volume, pressure dependence of the magnetic properties, the relative energy of compounds in different crystal structures, and the relative energy of different spin orderings.

In this paper we present a study of the electronic structure and magnetic properties of all Y-Fe binary compounds by means of *ab initio* self-consistent band-structure calculations. In the series Y_2Fe_{17} – Y_6Fe_{23} – YFe_3 – YFe_2 the average magnetic moment per Fe atom is observed to decrease. Contrary to the Y-Co compounds, the Curie temperature is observed to increase with increasing Y concentration, from 310 K for Y_2Fe_{17} to 537 K for YFe_2 . Our aim is to investigate the predictive quality of the calculations, particularly with respect to the magnetic moments.

This work has been stimulated by recent developments in the search for novel materials for permanent magnets. After the development of excellent permanent magnets based on the intermetallic compound $Nd_2Fe_{14}B$,^{8,9} an intensive search for other Fe-rich rare-earth-containing intermetallic compounds has started.

Several groups investigated the possibilities of preparing novel binary rare-earth-iron compounds in crystal structures that occur in the rare-earth-manganese or rare-earth-cobalt system, but not in the rare-earth-iron system itself. A very promising new class of compounds was found by de Mooij and Buschow,¹⁰ who stabilized iron-rich compounds RFe_{12} in the tetragonal $ThMn_{12}$ structure by substituting some Ti, V, Cr, Mo, W, or Si for Fe, and independently by Ohashi *et al.*, who prepared the

compound $\text{SmFe}_{11}\text{Ti}$.¹¹ Band-structure calculations of hypothetical YFe_{12} and of transition-metal-substituted compounds will be reported in a separate paper.¹² Fe-rich rare-earth-iron compounds with the tetragonal BaCd_{11} structure,¹³ the tetragonal CeMn_6Ni_5 structure,¹⁴ and the distorted cubic NaZn_{13} structure¹⁵ have also been prepared by partial substitutions for the Fe atoms. Other methods were used for the preparation of SmFe_5 and NdFe_5 in the hexagonal CaCu_5 structure. SmFe_5 , stabilized by a small amount of oxygen or titanium, was prepared by sputtering onto a heated substrate,¹⁶ while metastable NdFe_5 was prepared by liquid quenching, using the melt-spinning technique.¹⁷ The CaCu_5 structure is closely related to the structures of the stable compounds YFe_3 and Y_2Fe_{17} . We have therefore included calculations of hypothetical YFe_5 in this paper.

II. CRYSTAL STRUCTURES

In Table I the crystallographic data used in the calculations are given. The crystal structures of YFe_2 , YFe_3 , YFe_5 , and Y_2Fe_{17} are closely related.¹⁸ The building blocks of these structures are shown in Fig. 1.

The hypothetical compound YFe_5 has the most simple structure. Its hexagonal CaCu_5 -type unit is identical to the building block in Fig. 1(a). There are two inequivalent Fe sites: the 2(c) sites within the plane contain-

ing the Y atoms, and the 3(g) sites in the top and bottom planes.

The cubic MgCu_2 Laves-phase structure of YFe_2 can be viewed as a stacking of the Y_2Fe_4 blocks in Fig. 1(b). One of the Fe atoms in the intermediate layer of the YFe_5 block is replaced by an Y atom and, to avoid too small interatomic distances, the Y atoms are shifted by $\frac{1}{8}c$ parallel to the c axis to opposite sides of the $Z = \frac{1}{2}c$ layer. The top layer is shifted by $\frac{1}{3}$ of the length of the diagonal of the basal plane. The stacking of these blocks is shown schematically in Fig. 1(c). Similarly, the rhombohedral structure of YFe_3 can be viewed as a repeated stacking of YFe_5 and Y_2Fe_4 blocks [Fig. 1(d)].

The structure of Y_2Fe_{17} follows from the CaCu_5 structure of YFe_5 by replacing one-third of the Y atoms by Fe pairs (so-called dumbbell pairs). Layers of YFe_5 units in which this has been done can be stacked basically in two different ways, leading to the rhombohedral $\text{Th}_2\text{Zn}_{17}$ structure [Fig. 1(e)] or to the hexagonal $\text{Th}_2\text{Ni}_{17}$ structure [Fig. 1(f)]. It is possible to prepare Y_2Fe_{17} in either of these structures,¹⁹ in which the local environments of the atoms are very similar. Mössbauer spectroscopy shows that the magnetic moments in these two modifications are also almost equal.²⁰ In view of the large size of the unit cell of the hexagonal modification (38 atoms/cell), we have restricted ourselves to the rhombohedral $\text{Th}_2\text{Zn}_{17}$ structure (with 19 atoms/cell).

TABLE I. Crystallographic data of Y-Fe compounds. [P. Villars and L. D. Calvert, *Pearson's Handbook of Crystallographic Data for Intermetallic Phases* (American Society of Metals, Metals Park, OH, 1985)].

Compound	Structure type and lattice parameters	Pearson symbol and space group	Atomic positions		
Y_2Fe_{17}	$\text{Th}_2\text{Zn}_{17}$ ($a = 8.46 \text{ \AA}$, $c = 12.41 \text{ \AA}$)	$hR 19$ ($R\bar{3}m$, No. 166)	Y	6(c)	$(0, 0, \frac{1}{3})$
			Fe(1)	6(c)	$(0, 0, 0.097)$
			Fe(2)	9(d)	$(\frac{1}{2}, 0, \frac{1}{2})$
			Fe(3)	18(f)	$(0.333, 0, 0)$
			Fe(4)	18(h)	$(\frac{1}{2}, \frac{1}{2}, 0.167)$
YFe_5^a	CaCu_5 ($a = 4.97 \text{ \AA}$, $c = 4.03 \text{ \AA}$)	$hP 6$ ($P6/mmm$, No. 191)	Y	1(a)	$(0, 0, 0)$
			Fe(1)	2(c)	$(\frac{1}{3}, \frac{2}{3}, 0)$
			Fe(2)	3(g)	$(\frac{1}{2}, 0, \frac{1}{2})$
Y_6Fe_{23}	$\text{Th}_6\text{Mn}_{23}$ ($a = 12.12 \text{ \AA}$)	$cF 116$ ($Fm\bar{3}m$, No. 225)	Y	24(e)	$(0.203, 0, 0)$
			Fe(1)	4(b)	$(\frac{1}{2}, \frac{1}{2}, \frac{1}{2})$
			Fe(2)	24(d)	$(0, \frac{1}{4}, \frac{1}{4})$
			Fe(3)	32(f ₁)	$(0.178, 0.178, 0.178)$
			Fe(4)	32(f ₂)	$(0.378, 0.378, 0.378)$
YFe_3	NbBe_3 ($a = 5.133 \text{ \AA}$, $c = 24.60 \text{ \AA}$)	$hR 12$ ($R\bar{3}m$, No. 166)	Y(1)	3(a)	$(0, 0, 0)$
			Y(2)	6(c)	$(0, 0, 0.1402)$
			Fe(1)	3(b)	$(0, 0, \frac{1}{2})$
			Fe(2)	6(c)	$(0, 0, 0.3344)$
			Fe(3)	18(h)	$(0.504, 0.496, 0.0818)$
YFe_2	Cu_2Mg ($a = 7.363 \text{ \AA}$)	$cF 24$ ($Fd\bar{3}m$, No. 227)	Y	8(a)	$(0, 0, 0)$
			Fe	16(d)	$(\frac{5}{8}, \frac{5}{8}, \frac{5}{8})$

^aEstimate of lattice parameters based on an interpolation of the concentration dependence of the Y-Fe compounds (see Sec. II).

The structure of Y_6Fe_{23} is not related to the structures mentioned above. The face-centered-cubic unit cell, which consists of 116 atoms, is quite complex. A peculiarity of the structure is the local surroundings of the Fe 4(b) atoms. The first eight nearest Fe neighbors form a coordination shell similar to that in bcc Fe, at a distance of 2.56 Å. However, the second-nearest neighbors are very far away (six Y atoms at 3.6 Å) and, consequently, the Fe 4(b) atoms are quite isolated.

In Fig. 2 the deviation of the average atomic volume from Vegard's law is plotted, which reflects the strength of the chemical bond. The figure shows a quite regular behavior with Y_6Fe_{23} as a notable exception. Its volume

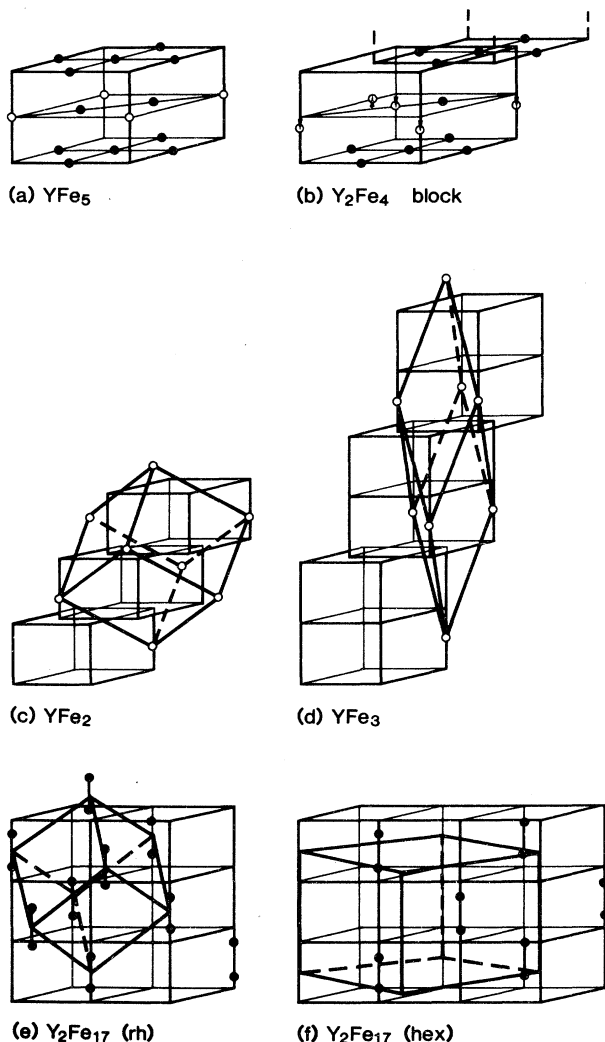


FIG. 1. Crystal structures of Y-Fe compounds. (a) Hexagonal unit cell of YFe_5 . Y and Fe atoms are drawn as open and solid spheres, respectively. (b) Y_2Fe_4 building block. (c) Stacking of Y_2Fe_4 blocks, and cubic unit cell of YFe_2 Laves-phase structure. (d) Alternative stacking of YFe_5 and Y_2Fe_4 blocks and rhombohedral unit cell of YFe_3 . (e) Dumbbell Fe pairs in rhombohedral Y_2Fe_{17} structure. (f) Dumbbell Fe pairs in hexagonal Y_2Fe_{17} structure.

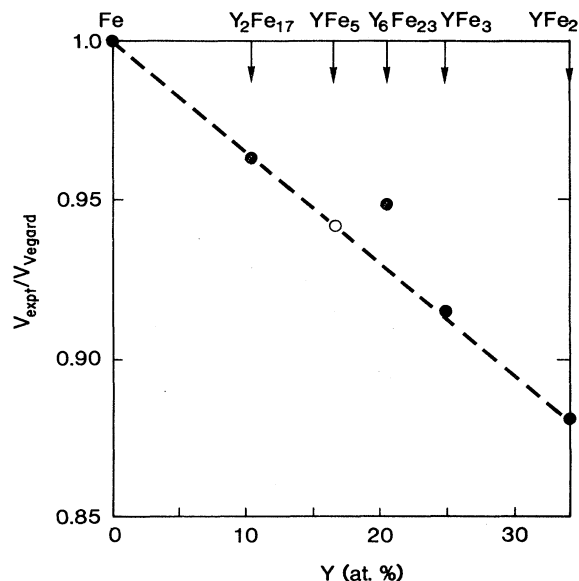


FIG. 2. Experimental volume of Y-Fe compounds relative to the volume according to Vegard's law. The open circle denotes the estimate of the volume of YFe_5 , based on an interpolation of the volumes of structurally related compounds (dashed line).

is approximately 2% larger than would follow from an interpolation, based on the volumes of the other compounds. Interpolation was used to estimate the volume of hypothetical YFe_5 (dashed line).

III. CALCULATIONAL METHOD

The band-structure calculations were performed using the augmented-spherical-wave (ASW) method.²¹ Exchange and correlation were treated within the local-spin-density-functional approximation, using the form given by von Barth and Hedin,²² with the parameters given by Janak.²³ The calculations were scalar relativistic, including mass-velocity and Darwin terms. Spin-orbit interaction was neglected.

Within the ASW method, the crystal is subdivided into overlapping Wigner-Seitz spheres, centered at the atomic positions. The potential in each of the spheres is assumed to be spherically symmetric. This overlapping-spheres approximation leads to a considerable reduction of the computational effort, compared to full-potential methods like the full-potential linear augmented-plane-wave (FLAPW) method.²⁴ In fact, full-potential calculations of the most complex Y-Fe compounds would cost an unrealistically large amount of computational time. In low-dimensional systems or open lattices this atomic-spheres approximation might cause severe errors. However, in the metals treated in this paper only small errors are expected, as the coordination numbers are high and the lattices do not contain large holes.

For calculations on elemental metals in which all sites are equivalent, the overlapping-spheres approximation does not introduce adjustable parameters because of the requirement that the volume of the spheres should be

equal to the volume per atom. However, for compounds a choice must be made for the radius ratio of the spheres on inequivalent sites. For all compounds we used the ratio $r_Y:r_{Fe}=1.35$. Using this value the overlap between the spheres around atoms on neighbor sites is generally of the order of 10–15% of the radius, as, for example, in fcc and bcc metals. We investigated the influence of the radius ratio on the calculated magnetic moments by additional calculations using the radius ratio $r_Y:r_{Fe}=1.25$.

The basis set of valence states used in the calculations was ($4s$, $4p$, and $3d$) for Fe and ($5s$, $5p$, and $4d$) for Y. In the calculation of the three-center overlap integrals the almost empty $4f$ states were also used. This can be regarded as treating these f states as a perturbation. The number of k points in the irreducible part of the Brillouin zone on which the calculation of the self-consistent potential was based could be much smaller for the systems with large unit cells than for systems with small unit cells. For YFe_2 , for example, we used 64 k points, while for Y_6Fe_{23} 10 k points were sufficient. Calculations with more k points did not change the calculated partial moments by more than $0.02\mu_B$. The density-of-states calculations were based on meshes of 1012, 4096, 280, 1300, and 2050 k points for Y_2Fe_{17} , YFe_5 , Y_6Fe_{23} , YFe_3 , and YFe_2 , respectively.

IV. RESULTS

A. Volume, bulk modulus, and heat of formation

From the total energy, calculated at different volumes, the equilibrium volumes, bulk moduli, and heats of formation (with respect to bcc Fe and hcp Y) were determined. In Table II the results are compared with the experimental data. The data within parentheses refer to a

radius ratio $r_Y:r_{Fe}=1.25$. If not stated otherwise, all other data and figures presented in this paper have been calculated using $r_Y:r_{Fe}=1.35$.

For all Y-Fe compounds the ferromagnetic calculations systematically result in a 6–7% lower volume than the experimental volume. A similar error was also found for elemental bcc Fe and hcp Y. A different choice of the radius ratio, $r_Y:r_{Fe}=1.25$, leads to a further reduction of the calculated volume, to approximately 8–10% below the experimental volume.

The calculated as well as the experimental bulk moduli show a decreasing tendency with increasing Y concentration. However, the bulk modulus of Y_6Fe_{23} is, theoretically and experimentally, slightly lower than the bulk modulus of the neighbor compounds Y_2Fe_{17} and YFe_3 . For the Fe-rich compounds, and for bcc Fe itself, the calculated bulk modulus is systematically too high. For YFe_2 and for hcp Y the difference between theory and experiment is within the experimental and calculational accuracy.

While the effect of the $r_Y:r_{Fe}$ ratio on the calculated equilibrium volume and bulk modulus is modest, Table II shows that the effect on the energy of formation is quite strong. The calculated total energy is approximately 100 meV lower with $r_Y:r_{Fe}=1.25$ than with $r_Y:r_{Fe}=1.35$. We found that a further reduction of $r_Y:r_{Fe}$ to values below 1.20 generally leads to an increase of the calculated total energy. The relative values of the calculated energies of different compounds do not correlate much with the experimental differences in the heat of formation, measured at 973 K, which are given in the last column of Table II. From the sensitivity of the calculated binding energy to the radius ratio, we conclude that for calculations of the phase stabilities, the approximations made within the ASW method are too crude.

TABLE II. Comparison of calculated volumes, bulk moduli, and heats of formation with experimental data. Numbers in parentheses were obtained from calculations using $r_Y:r_{Fe}=1.25$.

	$V_{\text{calc}}/V_{\text{expt}}$	B_{calc}^a (Mbar)	B_{expt} (Mbar)	$E_{\text{calc}}(0\text{ K})^b$ (meV/atom)	$\Delta H_{\text{expt}}(973\text{ K})^c$ (meV/atom)
Fe (bcc)	0.939	2.3	1.7	0	0
Y_2Fe_{17} (rhombohedral)	0.933 (0.916)	1.6 (1.3)	1.3 ^f	42 (-38)	-66
YFe_5	0.935 ^d (0.924)	1.5 (1.5)		-74 (-140)	
Y_6Fe_{23}	0.935 (0.900)	1.2 (1.1)	1.0 ^f	71 (-69)	-84
YFe_3	0.935 (0.910)	1.3 (1.1)	1.1 ^f	-26 (-150)	-93
YFe_2	0.935 (0.914)	1.3 (1.3)	1.29 ^f	24 (-101)	-74
Y ^e	0.936	0.43	0.45	0	0

^aAccuracy $\pm 10\%$.

^bEstimated uncertainty due to finite number of k points is ± 15 meV/atom.

^cP. R. Subramanian and J. F. Smith, CALPHAD 8, 295 (1984).

^dEstimate of V_{expt} (See Fig. 2).

^eASW calculation of hcp Y with $c/a = 1.593$.

^fData for Er-Fe compounds, M. Brouha, K. H. J. Buschow, and A. R. Miedema, IEEE Trans. Magn. MAG-10, 182 (1974).

B. Average magnetic moment

Figure 3 shows the volume dependence of the average moment per Fe atom. In Fig. 4 the calculated moments at the calculated volume (indicated by crosses in Fig. 3), the calculated moments at the experimental volume and the experimental moments are given. Table III contains the numerical data and references.²⁵⁻³¹ Note that the experimental moments are the total moments, including the orbital contribution to the moment, while the calculations yield only the spin contribution. For Fe the orbital moment is known to be $0.09\mu_B$,³² but for the Y-Fe compounds no measurements of the g factor, from which the orbital moment can be derived, have been published. A calculation by Szpunar³³ indicates that in Y_2Fe_{17} the average orbital moment is approximately $0.03\mu_B$. The anisotropy of the magnetic moment of Y_2Fe_{17} that was measured by Sinnema²⁶ ($2.07\mu_B$ for the field along the a or b axis and $2.03\mu_B$ with the field along the c axis) indicates that the orbital moment is at least $0.04\mu_B$.

The moments that were calculated at the calculated volume are $0.06\mu_B$ – $0.22\mu_B$ smaller than the total experimental moments μ_{expt} and the moments that were calculated at the experimental volume are almost identical to μ_{expt} (Y_2Fe_{17}) up to at most $0.14\mu_B$ higher than μ_{expt} . If we assume that the average orbital moment is $0.05\mu_B$ – $0.10\mu_B$ per Fe atom, then the moments calculated at V_{calc} are in better agreement with the experimental spin moments than the moments which were calculated at V_{expt} . However, in the series YFe_2 – YFe_3 – Y_6Fe_{23} – Y_2Fe_{17} the difference between $\mu_{\text{calc}}(V_{\text{calc}})$ and μ_{expt} increases. This could indicate that the orbital moment increases in these series. A decrease of the $r_Y:r_{Fe}$ ratio to 1.25 leads to a small decrease of the average mo-

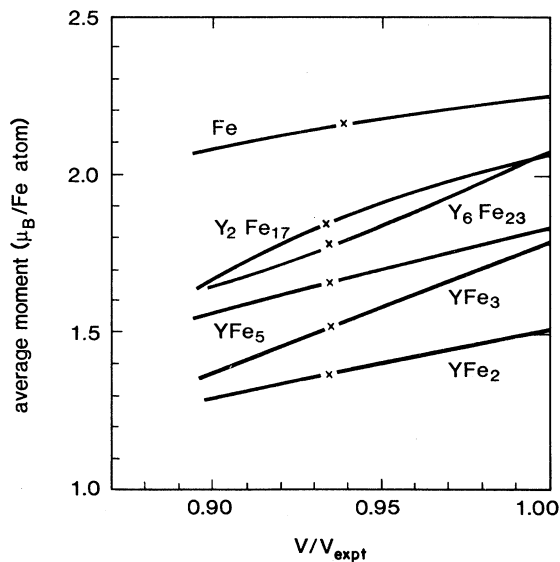


FIG. 3. Volume dependence of the average magnetic moment per Fe atom. Crosses denote the moment at the calculated equilibrium volume.

ments that were calculated at the (new) calculated equilibrium volume V_{calc} . This decrease is due to the decrease of V_{calc} , because calculations for a fixed volume show an increase in m_{calc} of approximately $0.05\mu_B$ upon decreasing $r_Y:r_{Fe}$ to 1.25.

Figure 3 shows that the stability of the magnetic moment against volume change varies strongly. For Fe the magnetization is much more stable than for Y_2Fe_{17} , Y_6Fe_{23} , and YFe_3 . In Sec. V we will discuss how $(\partial\bar{m}/\partial V)$ is related to the density of states at the Fermi level.

In addition to calculations for the ferromagnetic state, we have also performed calculations for the hypothetical nonmagnetic state. In Table IV some of the results are given. The nonmagnetic state is different from the paramagnetic state, in which there are finite moments which fluctuate in size and direction, without long-range ordering. Therefore, the energy difference between the ferromagnetic and nonmagnetic states (second column, Table IV) is not a proper measure for the temperature stability of the ferromagnetic state. Nevertheless, it is interesting to note that this energy difference is much higher in Fe ($T_c = 1044$ K) than in the Y-Fe compounds, which all have a much lower Curie temperature (highest $T_c = 537$ K for YFe_2). The volume difference between the

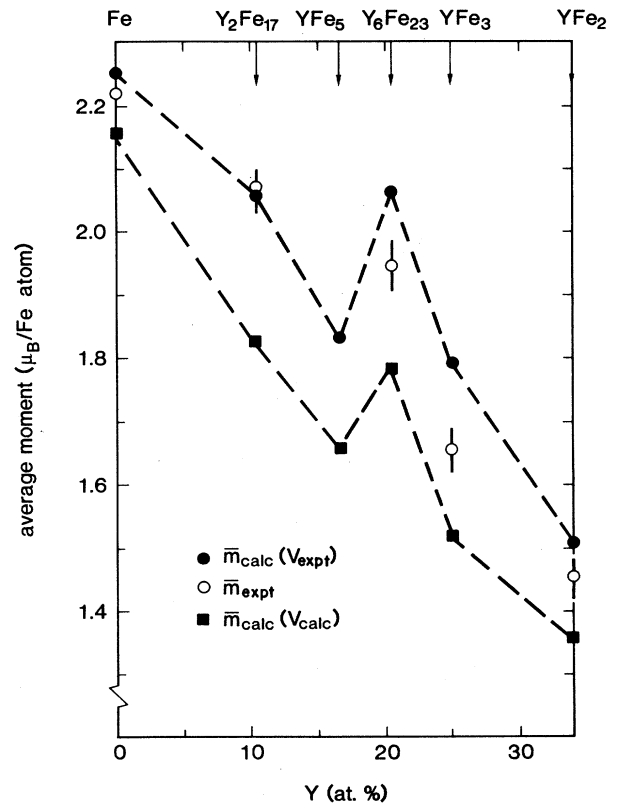


FIG. 4. Calculated moments at the calculated volume [$\bar{m}_{\text{calc}}(V_{\text{calc}})$], calculated moments at the experimental volume [$\bar{m}_{\text{calc}}(V_{\text{expt}})$], and experimental moment \bar{m}_{expt} . For numerical data and references, see Table III.

TABLE III. Calculated magnetic properties and experimental magnetic moments. Data between parentheses refer to calculations with $r_Y:r_{Fe}=1.25$. The uncertainties in the experimental moments reflect the experimental accuracies, as well as spread in the literature values.

	$\bar{m}_{\text{calc}}(V_{\text{calc}})$ ($\mu_B/\text{Fe-atom}$)	$\bar{m}_{\text{calc}}(V_{\text{expt}})$ ($\mu_B/\text{Fe-atom}$)	\bar{m}_{expt} ($\mu_B/\text{Fe-atom}$)	References \bar{m}_{expt}
Fe	21.6	2.25	2.22±0.01	25
Y ₂ Fe ₁₇ (rh)	1.83 (1.79)	2.06 (2.09)	2.07±0.03	26,27
YFe ₅	1.66 (1.67)	1.83 (1.88)		
Y ₆ Fe ₂₃	1.78 (1.77)	2.07 (2.13)	1.94±0.04	27,28,29
YFe ₃	1.52 (1.48)	1.79 (1.85)	1.65±0.04	27,30
YFe ₂	1.36 (1.34)	1.51 (1.56)	1.45±0.02	27,31

ferromagnetic and nonmagnetic states decreases with decreasing average Fe moment, with the exception of Y₆Fe₂₃, in which the difference is higher than expected from an interpolation of the values for the neighbor compounds YFe₅ and YFe₃ (5.7% versus 4.0% and 3.2%, respectively). While the volume of ferromagnetic Y₆Fe₂₃ is 2% larger than the volume that would be expected from an interpolation between the other members of the Y-Fe series (Fig. 2), we see that this volume anomaly is absent for nonmagnetic Y₆Fe₂₃. The relatively high average moment, the low bulk modulus, and the volume anomaly, all predicted well by the calculations, are interrelated. As to the bulk modulus, this is demonstrated by the last column of Table IV, which shows that also in this respect nonmagnetic Y₆Fe₂₃ behaves regularly.

For hypothetical YFe₅ the calculated moments are slightly lower than one would expect from an interpolation between the structurally related compounds YFe₃ and Y₂Fe₁₇. From the trend in the relative position of the experimental and calculated moments, we estimate that in YFe₅ the average moment per Fe atom is $(1.8\pm 0.07)\mu_B$, corresponding to a saturation magnetization of 1.22 ± 0.05 T.

C. Total densities of states

In Figs. 5(a)–5(f) the total densities of states are shown, calculated at the theoretical volume. All Y-Fe com-

TABLE IV. Calculated energy difference between the ferromagnetic and nonmagnetic states ($E_F - E_{NM}$), relative volume difference ($(V_F - V_{NM})/V_{\text{expt}}$), and bulk modulus of the nonmagnetic state.

	$-(E_F - E_{NM})$, (meV/Fe-atom)	$(V_F - V_{NM})/V_{\text{expt}}$	B_{NM} (Mbar)
Fe	295	0.061	3.0
Y ₂ Fe ₁₇ (rh)	79	0.049	2.1
YFe ₅	137	0.040	2.0
Y ₆ Fe ₂₃	47	0.057	1.8
YFe ₃	98	0.032	1.8
YFe ₂	125	0.026	1.6

pounds, as well as Fe itself, can be classified as weak ferromagnets, because in none of the compounds the majority-spin band is occupied completely. The DOS of Y₂Fe₁₇ and YFe₅ shows some similarity to the DOS of Fe. In both compounds, as well as in Fe, the majority- and minority-spin Fermi levels are situated above and below, respectively, of a pronounced peak of antibonding states. The densities of states of YFe₃, YFe₂, and, in particular, of Y₆Fe₂₃, are more complex. For these compounds a description of the spin splitting within the rigid-band model is a bad approximation. The majority-spin DOS of these compounds does not show a pronounced deep valley separating bonding and antibonding states, while in the minority-spin DOS such a valley is clearly present around the Fermi level. Such a local minimum in the DOS around the Fermi level, which can only be described well by self-consistent calculations, leads to an energetically more stable ground state.

D. Local moments and local densities of states

In Table V the calculated local moments are compared with the nuclear hyperfine fields, measured by ⁵⁷Fe Mössbauer spectroscopy, and with moments that were measured by neutron diffraction. To our knowledge, neutron-diffraction experiments were only reported for Y₆Fe₂₃. For this compound, the neutron data and the calculated moments agree very well, apart from a systematic difference of approximately $0.08\mu_B/\text{atom}$. From Mössbauer spectroscopy indirect information about the local moment can be obtained from the hyperfine fields. In the Y-Fe series Gubbens *et al.*³⁴ found an almost constant conversion factor from the average hyperfine field to the average magnetic moment per Fe atom of 14.8 T/ μ_B . In Table V we have applied this factor to the individual sites.^{35,36} The difference from the calculated moments is $(0.1-0.4)\mu_B/\text{atom}$, which is of the same order as the differences between the moments within one compound. For Y₆Fe₂₃ the neutron-diffraction data agree better with the calculations than the moments derived from Mössbauer spectroscopy. This indicates that a constant conversion factor of the hyperfine fields to the local

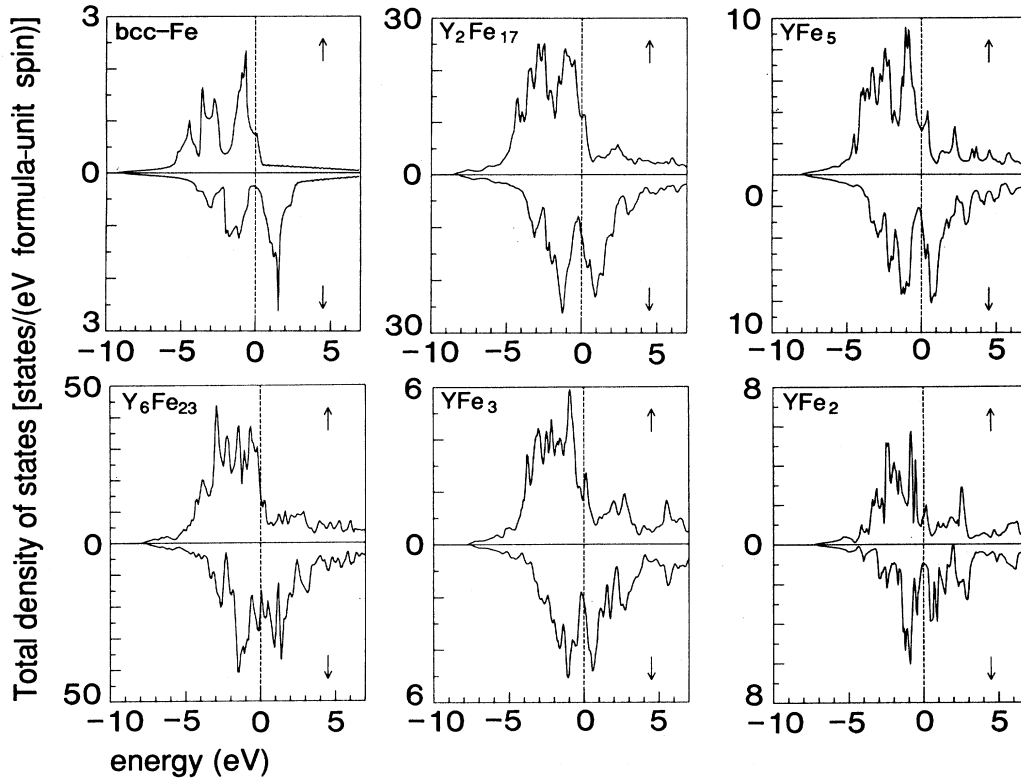


FIG. 5. Total density of states for majority-spin (\uparrow) and minority-spin (\downarrow) electrons of Fe and Y-Fe compounds. The energy is given with respect to the Fermi level (vertical dashed line).

TABLE V. Calculated and experimental moments at crystallographically inequivalent sites.

Compound	Site	$m_{\text{calc}}(V_{\text{expt}})$ (μ_B)	$m_{\text{calc}}(V_{\text{calc}})$ (μ_B)	Mössbauer spectroscopy ^a		Neutron diffraction ^c m (μ_B)
				H_f (T)	m (μ_B) ^b	
Y ₂ Fe ₁₇	Y 6(c)	-0.29	-0.20	36.4	2.46	
	Fe(1) 6(c)	2.29	2.12			
	Fe(2) 9(d)	1.91	1.60			
	Fe(3) 18(f)	2.25	2.08			
	Fe(4) 18(h)	1.97	1.67			
YFe ₅	Y 1(a)	-0.32	-0.24			
	Fe(1) 2(c)	2.10	2.00			
	Fe(2) 3(g)	1.78	1.53			
Y ₆ Fe ₂₃	Y 24(e)	-0.38	-0.32	37.0	2.50	2.16
	Fe(1) 4(b)	2.27	2.07			
	Fe(2) 24(d)	1.91	1.53			
	Fe(3) 32(f1)	2.16	1.82			
	Fe(4) 32(f2)	2.35	2.15			
YFe ₃	Y(1) 3(a)	-0.38	-0.28	22.2	1.50	
	Y(2) 6(a)	-0.45	-0.36			
	Fe(1) 3(b)	1.81	1.69			
	Fe(2) 6(c)	2.12	1.85			
	Fe(3) 18(h)	1.83	1.53			
YFe ₂	Y 8(a)	-0.53	-0.44	21.0	1.42	
	Fe 16(d)	1.78	1.58			

^aReferences 20, 34, and 35.

^bConversion factor from hyperfine field to moment: 14.8 T/ μ_B .

^cData for Y₆Fe₂₃ from Ref. 6.

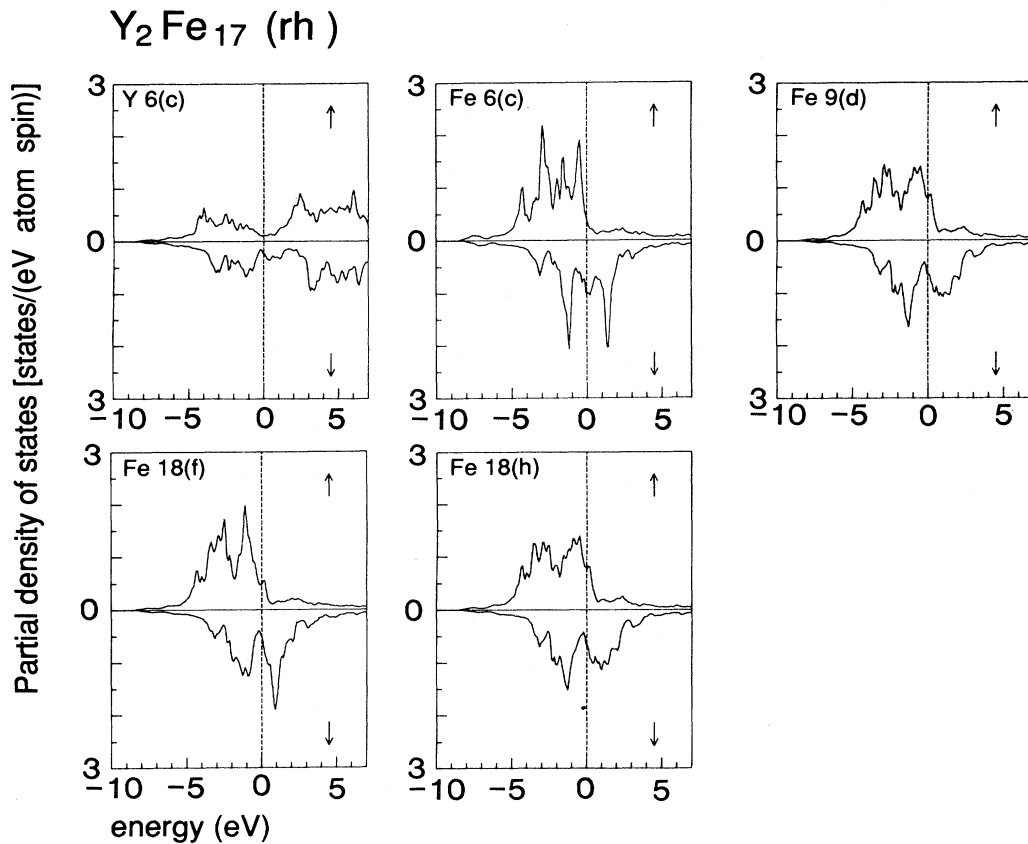


FIG. 6. Partial densities of states of inequivalent atoms in Y_2Fe_{17} .

moments is not a good approximation.

For all compounds we find a small moment on the Y site, which is coupled antiparallel to the Fe moments. It increases with increasing Y content, from $0.20\mu_B$ in Y_2Fe_{17} to $0.44\mu_B$ in YFe_2 . For YFe_2 the large antiparallel Y moment was already found by Mohn and Schwarz.⁷ They interpreted the effect as arising from covalent bond-

ing between the Fe and Y states. This covalent Fe-Y interaction causes the failure of the rigid-band model that was already noted in the discussion of the total densities of states in Sec. IV B. Whereas the Fe moments are localized, the spin density around the Y atoms is small and quite extended, which makes it difficult to determine the Y contribution to the magnetization density experimen-

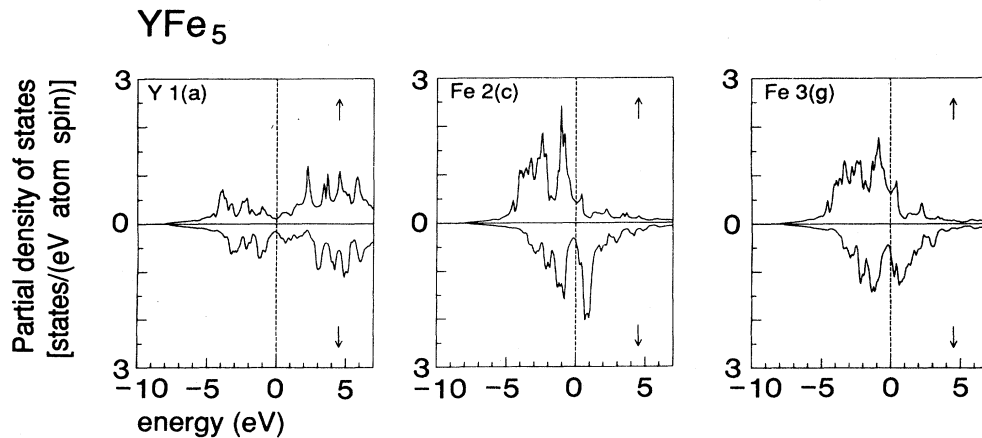


FIG. 7. Partial densities of states of inequivalent atoms in YFe_5 .

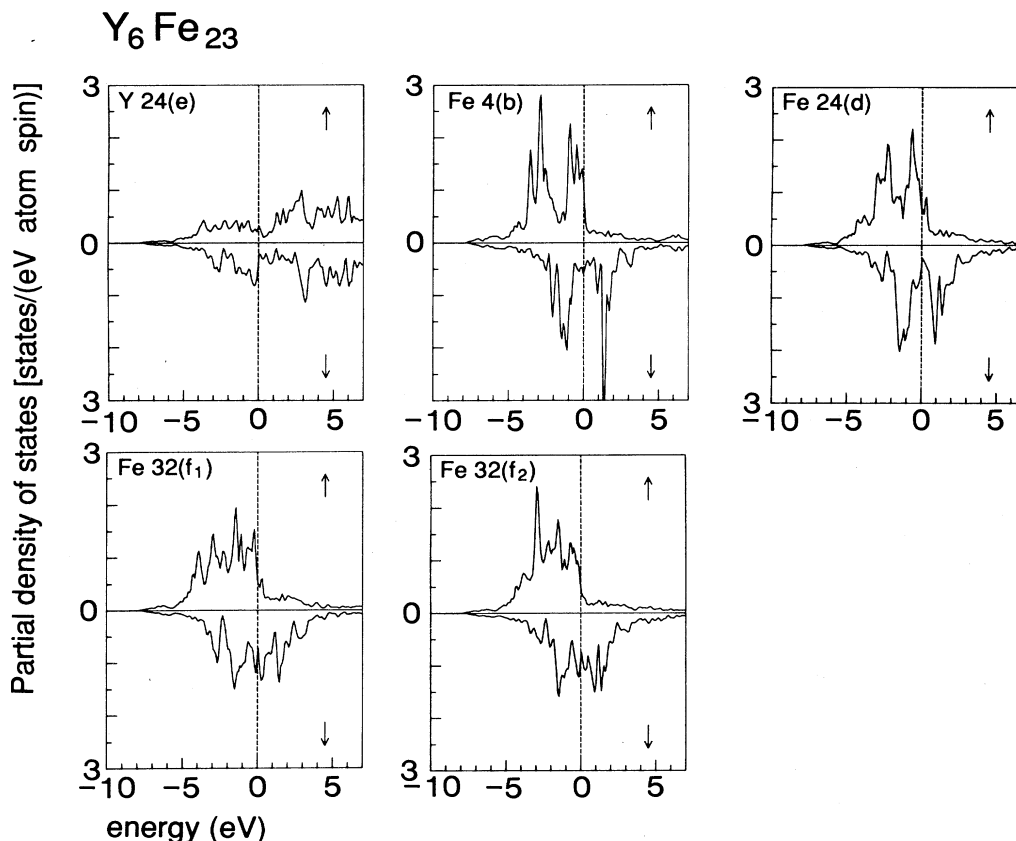


FIG. 8. Partial densities of states of inequivalent atoms in Y_6Fe_{23} .

tally. Experimental evidence of the induced moments on the Y site was provided by nuclear-hyperfine-field measurements by NMR (Ref. 37) and Mössbauer spectroscopy.³⁸

For hypothetical YFe_5 no comparison of the calculated local moments with experimental data is possible. However, due to the close structural relationship with Y_2Fe_{17} , the 2(c) sites in YFe_5 have a similar atomic surrounding to the 18(f) sites in Y_2Fe_{17} . The same holds for the 3(g) site in YFe_5 and the 9(d) and 18(h) sites in Y_2Fe_{17} . These similarities are reflected clearly in the sizes of the local moments.

In Figs. 6–10 the partial densities of states (DOS) for all crystallographically inequivalent sites in Y_2Fe_{17} , YFe_5 , Y_6Fe_{23} , YFe_3 , and YFe_2 , respectively, are shown. For all Fe atoms, with the exception of the atoms on the 6(c) sites of Y_2Fe_{17} and the 4(b) sites of Y_6Fe_{23} , the majority-spin DOS shows a pronounced peak just above the Fermi level. All these sites, for which the majority-spin band is not occupied completely, contribute to the weak ferromagnetic character of the Y-Fe compounds. For Y_2Fe_{17} and YFe_5 the antibonding peak in the partial DOS is quite narrow and high for the sites with a large local moment [6(c) and 18(f) in Y_2Fe_{17} and 2(c) in YFe_5], but broader and lower for the sites with smaller local moments. For Y_6Fe_{23} the peak structure of the antibonding

band is quite complex. For the (d), (f₁) and (f₂) sites the minority-spin Fermi level is located just above a steep edge in the DOS. For the majority-spin Fermi level this holds for all sites, including the (b) site. The partial DOS of the latter site shows some very sharp and narrow peaks, corresponding to rather localized states at these relatively isolated atoms (see Sec. II). In YFe_3 the Y atoms at the 6(c) sites are situated in the Y_2Fe_4 blocks (Fig. 1). Therefore, the partial DOS at these sites shows a strong similarity to the DOS of the Y [8(a)] sites of YFe_2 . The Y atoms at the 3(a) sites in YFe_3 are situated in the YFe_5 blocks. However, the similarity of their partial DOS with the DOS at the Y [1(a)] site in YFe_5 is quite poor. This can be explained by the presence of two Y nearest neighbors at 3.44 Å from the 3(a) sites in YFe_3 , while in YFe_5 the Y atoms are surrounded completely by Fe atoms.

V. DISCUSSION

A. Total magnetization

From the results presented in Sec. IV a coherent picture is obtained of the possibilities for predicting the electronic structure and magnetic properties of Y-Fe compounds by ASW calculation. Trends in the volume, the

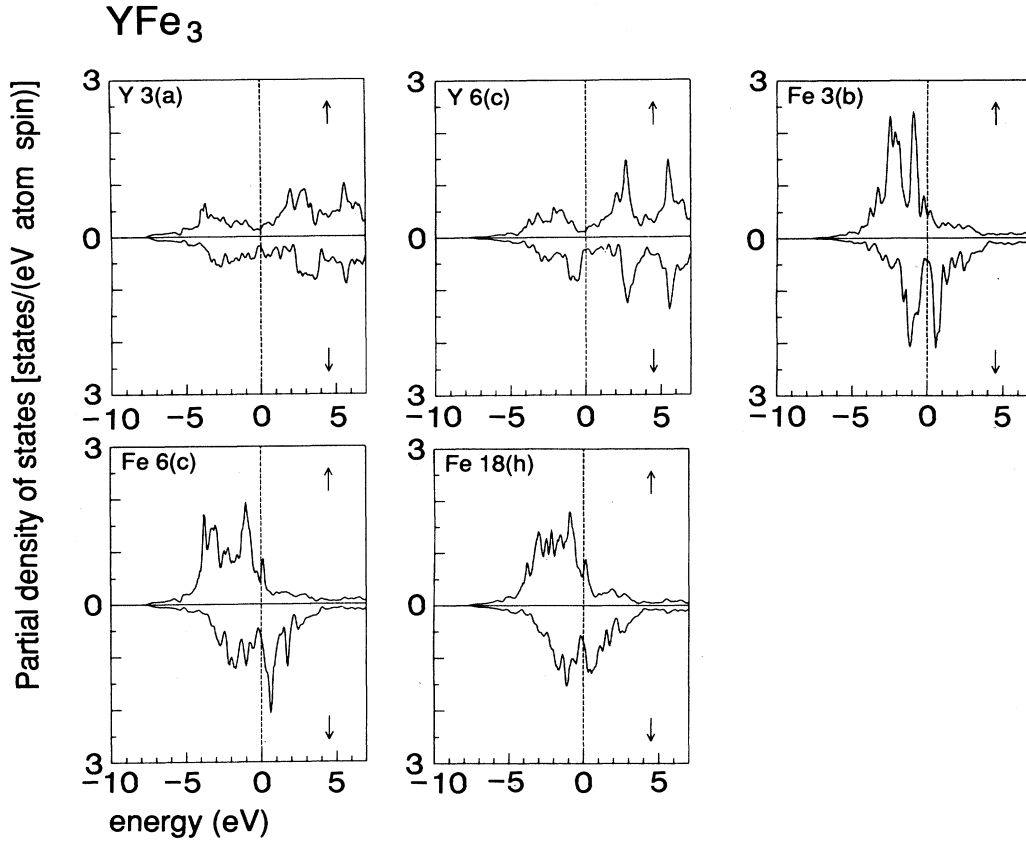


FIG. 9. Partial densities of states of inequivalent atoms in YFe₃.

bulk modulus, and the magnetic moments are predicted very well, including the anomalous values for Y₆Fe₂₃. The calculated values of the average magnetic moments at the calculated volume are $(0.1-0.2)\mu_B/\text{Fe-atom}$ lower than the experimental values. The remaining differences might be (partly) due to the neglect of the orbital contribution to the moment.

The calculated equilibrium volume is for all compounds approximately 6–7% too low, and, related to the volume error, the bulk moduli are too large. It is remarkable that the error in the calculated volume is quite independent of the particular compound. For bcc Fe, as well as for Y metal the error is 6–6.5%. Using the ASW method, we find that within the 4d series the calculated volume is within 1% of the experimental volume for the elements Nb to Pd, and 3% lower than the experimental volume for Zr. A similar result was obtained by the Korringa-Kohn-Rostoker (KKR) calculations, performed by Moruzzi *et al.*³⁹ From full-potential calculations on hcp Y, performed by Daalderop,⁴⁰ it was shown that the volume error is not related to the spherical approximation. The volume calculated in these calculations was 7% lower than the experimental value. Furthermore, it was found that by calculations using the linear muffin-tin-orbital (LMTO) method, in which (unlike the ASW method) the rigid-core approximation was made, the volume of hcp Y is underestimated by only 3%. With respect to the valence-electron electronic structure, the LMTO method is quite similar to the ASW method. From these results we conclude that it would be of interest to examine the role of the core levels in determining the total energy in more detail.

From the results of calculations of bcc Fe by Hathaway *et al.*⁴¹ it can be concluded that another part of the

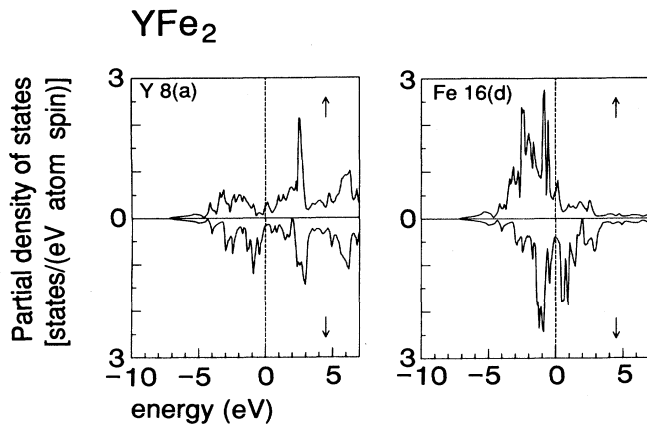


FIG. 10. Partial densities of states of inequivalent atoms in YFe₂.

systematic volume error is due to the use of the local-spin-density approximation, within which exchange and correlation effects in magnetic $3d$ -transition-metal atoms are treated incorrectly. They found that also in calculations without any approximation to the shape of the potential, using the same form of the exchange-correlation potential as we have used in the present paper, the volume of bcc Fe is underestimated. In the full-potential calculations the volume was underestimated by 10%, and the calculated spin magnetic moment was $(2.06 \pm 0.01)\mu_B$. Since in the ASW calculations the volume error is only 6% and the calculated spin magnetic moment is $2.16\mu_B$, it can be concluded that in the case of bcc Fe the use of the overlapping-spheres approximation leads to a partial compensation for the volume error, and a slight overcompensation of the error in the spin magnetic moment whose experimental value is $2.12\mu_B$. They also performed calculations with a different type for the exchange-correlation potential, which was introduced by Vosko, Wilk, and Nusair,⁴² and which is generally regarded as the potential which yields the most accurate description for the charge- and spin-density-dependent energy of the homogeneous electron gas. However, these calculations resulted in even larger deviations from the experiment properties: $V_{\text{calc}}/V_{\text{expt}} = 0.895$ and $V_{\text{spin}} = 2.18\mu_B$. These results, as well as calculations of the shape of the Fermi surface,⁴² calculations of the relative stability of fcc Fe and bcc Fe,^{43,44} and calculations for other elements,³⁹ illustrate the shortcomings of the local-spin-density-functional theory in describing accurately the properties of magnetic $3d$ metals. Model calculations on Fe, Co, and Ni show indeed that a proper inclusion of on-site correlation leads to a significant correction for the calculated lattice constants.⁴⁵

The total error in the calculated volume is then a sum of contributions of the Fe sublattice, and of the Y sublattice, which with increasing Y concentration are decreasing and increasing, respectively. It is expected that a better value for the calculated spin magnetic moment is obtained from a calculation at the volume V'_{calc} , which would have been obtained in the absence of the error in the Y volume. Since $V'_{\text{calc}} > V_{\text{calc}}$, this could lead to a significantly better agreement between \bar{m}_{calc} and \bar{m}_{expt} , in particular, for the compounds which have the highest Y concentrations.

If it is assumed that the volume error due to the Y sublattice is simply proportional to the partial Y volume, calculated using the atomic radii that were used in the ASW calculations, then $V'_{\text{calc}} \approx 0.970V_{\text{expt}}$ and $\bar{m}_{\text{calc}} = 1.44\mu_B/\text{Fe-atom}$ for YFe_2 , e.g., which is very close to the experimental moment $\bar{m}_{\text{expt}} = 1.45\mu_B/\text{Fe-atom}$. Of course the correction of the calculated volume would also lead to a correction of the local moments and of the total and partial density of states.

B. Influence of sphere radii

In ASW calculations for compounds the choice of the radius ratio of inequivalent atoms influences the results. As discussed in Sec. III, we have chosen equal volumes for all inequivalent Fe atoms, and for all inequivalent Y

atoms. For Y and Fe atoms a radius ratio of the Wigner-Seitz spheres of 1.35 was used. A comparison with calculations using $r_Y:r_{\text{Fe}} = 1.25$ shows that the results are slightly dependent on the radius ratio. For $r_Y:r_{\text{Fe}} = 1.25$ the volume underestimation is somewhat larger (8–9%), but for the calculated moments at the calculated volumes the differences are less than $0.05\mu_B/\text{Fe-atom}$. The moments, calculated at the experimental volume, are approximately $0.05\mu_B/\text{Fe-atom}$ larger. The calculated total energy is extremely sensitive to the choice of the sphere radii. This result shows that for lattice-stability calculations a full-potential approach is necessary. However, we remark that the order of magnitude of the calculated energy of formation, being 50–100 meV/atom, is predicted quite well if we take $r_Y:r_{\text{Fe}} = 1.35$ and $r_Y:r_{\text{Fe}} = 1.25$. Compared to the heat of formation of Y-Co and Y-Ni compounds, which can be estimated from experimental data for La-Co, Th-Co, La-Ni, and Th-Ni (Ref. 46) to be of the order 200 and 400 meV/atom, respectively, for the 1:1 compound, the values for the Y-Fe compounds are relatively small.

C. Density of states

The total density-of-states curves for Y_2Fe_{17} , Y_6Fe_{23} , and YFe_3 agree with those, calculated by Inoue and Shimizu,³ with respect to the position of the majority-spin Fermi level, which is situated in a valley of the DOS, just below a narrow peak at the upper edge of the d band. Apart from this similarity, the shapes of the two sets of DOS curves differ drastically. This results, for example, in important differences in the local densities of states at the Fermi level, but in spite of this, in most cases the calculated local moments do not differ very much (see Table VI). The ASW calculations generally yield lower values for the local densities of states at the Fermi level, particularly for the minority-spin electrons. The difference can be explained by considering that an adjustment of the potential resulting in a lowering of the density of states at the Fermi level, and thereby resulting in a decrease of the total energy, is only possible in a self-consistent calculation. The importance of this effect can be judged from a comparison of the majority and minority density-of-states curves in Figs. 5–10. From these curves it is clear that a rigid spin splitting of the density of states, as used by Inoue and Shimizu, is not a good approximation. Another approximation which influences the shape of their DOS curves is the neglect of the hybridization with the s/p band.

D. Volume dependence of magnetic moments

The volume dependence of the magnetization is fairly weak for Fe and YFe_2 , but much stronger and more non-linear for Y_2Fe_{17} and Y_6Fe_{23} (see Fig. 3). Within the Stoner model (exchange splitting Δ proportional to the magnetic moment m : $\Delta = Im$, with I the effective exchange integral), and assuming the following: (i) the $3d$ -band width is inversely proportional to the fifth power of the lattice constant, (ii) the d band deforms uniformly under pressure, and (iii) I is independent of the volume, it

TABLE VI. Comparison of local densities of states at the Fermi level and local magnetic moments obtained in the present work and in the work by Inoue and Shimizu (Ref. 3) (IE). Units of $N(\epsilon_F)$: $\text{eV}^{-1} \text{atom}^{-1} \text{spin}^{-1}$.

	Site	$N(\epsilon_F, \uparrow)$		$N(\epsilon_F, \downarrow)$		$M (\mu_B)$	
		Present work	IE	Present work	IE	Present work	IE
Y_2Fe_{17}	Y	0.11		0.24		-0.20	
	Fe(1)	0.38	0.40	1.15	0.98	2.12	2.31
	Fe(2)	0.77	1.18	0.73	0.90	1.60	1.55
	Fe(3)	0.47	1.02	0.52	1.14	2.08	1.86
	Fe(4)	0.76	1.18	0.72	1.14	1.67	1.79
YFe_5	Y	0.10		0.16		-0.24	
	Fe(1)	0.41		0.38		2.00	
	Fe(2)	0.62		0.58		1.53	
Y_6Fe_{23}	Y	0.36		0.30		-0.32	
	Fe(1)	0.82	1.14	0.65	0.55	2.07	2.19
	Fe(2)	0.66	1.14	0.36	0.98	1.53	2.10
	Fe(3)	0.54	0.57	0.86	1.34	1.82	1.68
	Fe(4)	0.49	0.69	0.90	1.83	2.15	2.10
YFe_3	Y(1)	0.13		0.20		-0.28	
	Y(2)	0.12		0.24		-0.36	
	Fe(1)	0.43	0.45	0.45	1.04	1.69	1.60
	Fe(2)	0.49	0.48	0.63	1.16	1.85	1.67
	Fe(3)	0.62	0.60	0.67	1.16	1.53	1.59
YFe_2	Y	0.25		0.18		-0.44	
	Fe	0.61	0.43	0.37	0.96	1.58	

can be shown that $\partial m / \partial V$ is related to the DOS at the Fermi level by

$$\frac{V}{m} \left[\frac{\partial m}{\partial V} \right]_{H=0} = \frac{5}{3} \frac{2I}{\left[\frac{1}{N(\epsilon_F, \uparrow)} + \frac{1}{N(\epsilon_F, \downarrow)} - 2I \right]} \quad (1)$$

(see Mathon, Ref. 47, Eq. 2.17, with I independent of the bandwidth).

Equation (1) shows that the volume dependence of the magnetization in strong ferromagnets [occupied d band, $N(\epsilon_F, \uparrow)$ small] is very small, while in weak ferromagnets, in which $N(\epsilon_F, \uparrow)$ and $N(\epsilon_F, \downarrow)$ can be high, $\partial m / \partial V$ is much higher. In some cases the denominator of the right-hand part of Eq. (1) can even go to zero, resulting in a singularity in $m(V)$. Moruzzi *et al.* have shown that this situation occurs in hypothetical fcc Fe.⁴⁸ The relatively strong nonlinearity of $m(V)$ in Y_2Fe_{17} and Y_6Fe_{23} can be explained by the rapid variation of the density of states close to the Fermi level [see Figs. 5(b) and 5(d)].

In the derivation of Eq. (1) it was assumed implicitly that there is only one atomic site per unit cell. Complications, like the presence of several inequivalent magnetic atoms, or the presence of nonmagnetic atoms, are not taken into account. Nevertheless, we have found that for the Y-Fe compounds the volume dependence of the local moments is described well by Eq. (1). This can be seen from Table VII, in which the $\partial m / \partial V$ values that were

calculated according to Eq. (1), using $I=0.925 \text{ eV}$,⁴¹ are compared with the $\partial m / \partial V$ values, found by calculations at different volumes. For bcc Fe the values $N(\epsilon_F, \uparrow) = 0.74 \text{ states (eV atom spin)}^{-1}$ and $N(\epsilon_F, \downarrow) = 0.25 \text{ states (eV atom spin)}^{-1}$ were used. The DOS data for the Y-Fe compounds were taken from Table VI.

The volume dependence of the average magnetic moment per Fe atom can be obtained in two ways from the DOS: (i) as the weighted average of the volume dependence of the local moments, and (ii) using Eq. (1) with $\bar{N}(\epsilon_F, \uparrow)$ and $\bar{N}(\epsilon_F, \downarrow)$, averaged over all Fe atoms. Using method (i) the local moments are regarded as being quite independent, while in method (ii) the presence of different localized moments is disregarded. Both methods can yield quite different results if for the different atoms in the crystal the $N(\epsilon_F)$ values are very dissimilar. In Table VII the $(V/\bar{m})(\partial \bar{m} / \partial V)$ values, calculated according to these two methods, are compared with the result obtained directly from a variation of the volume. Apparently, the results of the two methods do not differ much in the cases considered and the agreement with the value obtained directly is quite good.

We conclude that trends in the volume dependence of the local and total moments can be understood well from the density of states at the Fermi level. Numerical differences between the values of $\partial m / \partial V$ obtained by Eq. (1) and the value obtained directly by a volume variation can be attributed to the neglect of the yttrium contribution to the moment and the DOS, to the numerical inac-

TABLE VII. Volume dependence of magnetic moments. Comparison of $(V/m)(\partial m/\partial V)$, calculated at V_{calc} , using Eq. (1), with values obtained directly from calculations at different volumes.

		$(V/m)(\partial m/\partial V)$ [Eq. (1)]	$(V/m)(\partial m/\partial V)$ (Direct calc.)	$(V/\bar{m})(\partial \bar{m}/\partial V)$ [Method (i)]	$(V/\bar{m})(\partial \bar{m}/\partial V)$ Method (ii)	$(V/\bar{m})(\partial \bar{m}/\partial V)$ (Direct calc.)
Fe	Fe(1)	0.88	0.85	0.88	0.88	0.85
Y ₂ Fe ₁₇	Fe(1)	1.9	2.1			
	Fe(2)	3.8	3.3	2.5	2.5	2.4
	Fe(3)	1.4	1.2			
	Fe(4)	3.6	3.3			
YFe ₅	Fe(1)	1.0	0.8	1.6	1.5	1.6
	Fe(2)	2.1	2.2			
Y ₆ Fe ₂₃	Fe(1)	3.4	3.3			
	Fe(2)	1.3	1.8			
	Fe(3)	2.6	1.8	2.3	2.4	2.6
	Fe(4)	2.4	2.2			
YFe ₃	Fe(1)	1.1	0.9			
	Fe(2)	1.7	2.0	2.2	2.1	2.6
	Fe(3)	2.6	3.1			
YFe ₂	Fe(1)	1.2	1.5	1.2	1.2	1.5

curacy of the calculated DOS values (errors of the order of 10%), and possibly to a small variation of I with the volume.

Experimental data on $\partial m/\partial V$ can be obtained either from direct measurements of the pressure dependence of the magnetization or from an indirect determination from the forced volume-magnetostriction coefficient h , which by a thermodynamic relation⁴⁵ can be related to $\partial m/\partial V$,

$$h \equiv \frac{1}{V} \left[\frac{\partial V}{\partial H} \right]_{T,p} = -\frac{1}{V} \left[\frac{\partial m}{\partial p} \right]_{T,H} = +\mu_0 \kappa \left[\frac{\partial m}{\partial V} \right]_{T,H} \quad (2)$$

On the right-hand side of this equation κ is the isothermal compressibility. For bcc Fe the experimental value of h is $5.6 \times 10^{-12} \text{ (A/m)}^{-1}$ (Ref. 49) and $\kappa = 5.9 \times 10^{-12} \text{ Pa}^{-1}$. A calculation of the dimensionless quantity $(V/m)(\partial m/\partial V)$ using Eq. (2) then yields a value of 0.43, while the theoretical value is 0.85.

For YFe₂ $h_{\text{expt}} = 5.6 \times 10^{-12} \text{ (A/m)}^{-1}$ (Ref. 50) and $\kappa_{\text{expt}} = 8.3 \times 10^{-12} \text{ Pa}^{-1}$, from which it follows that $(V/m)(\partial m/\partial V)$ is 1.33, while the theoretical value is 1.5. From the comparison between theoretical and experimental values of $(V/m)(\partial m/\partial V)$ of Fe and YFe₂, no general conclusion can be obtained about the accuracy of the calculated values. Unfortunately, no experimental data for the other Y-Fe compounds are available.

VI. CONCLUSIONS

In this paper we have presented the results of self-consistent *ab initio* band-structure calculations of the Y-

Fe compounds. The calculated magnetic moments agree well with the experimental data, if the presence of a small orbital contribution to the total moment is assumed. Measurements of the orbital moment would contribute significantly to a more detailed evaluation of the accuracy of the computational methods used.

In the case of Y₆Fe₂₃ the local magnetic moments on the four inequivalent Fe sites can be compared with neutron-diffraction data. The agreement is very good, while the agreement with the moments derived from the nuclear hyperfine fields, which were determined by Mössbauer spectroscopy, is worse. In order to get a more general picture of the situation, neutron-diffraction determinations of the local moments of Y₂Fe₁₇ and YFe₃ would be helpful.

A unique feature of self-consistent *ab initio* calculations is the possibility of calculating the volume dependence of several physical quantities. From the volume dependence of the total energy the equilibrium volume and the bulk modulus were derived. The calculated equilibrium volume is systematically 6–7% too small. This was attributed to (i) a failure of the local-spin-density-functional approximation in describing the contribution of the Fe sublattice to the total volume, and (ii) an error in the contribution of the Y sublattice. The calculated volume dependence of the local and total magnetic moments could be related in a simple way to the density of states at the Fermi level. Experimental determinations of the volume dependence of the magnetization of the Y-Fe compounds are necessary to judge the validity of our predictions.

- ¹K. H. J. Buschow, Rep. Prog. Phys. **40**, 1179 (1977); K. H. J. Buschow, *Ferromagnetic Materials*, edited by E. P. Wohlfahrt (North-Holland, Amsterdam, 1980), Vol. 1, p. 297.
- ²I. A. Campbell, J. Phys. F **2**, L47 (1972).
- ³J. Inoue and M. Shimizu, J. Phys. F **15**, 1511 (1985); J. Inoue, Physica B+C **149B**, 376 (1988), and references therein.
- ⁴M. Shimizu, J. Inoue, and S. Nagasawa, J. Phys. F **14**, 2673 (1984).
- ⁵H. Yamada, J. Inoue, K. Terao, S. Kanda, and M. Shimizu, J. Phys. F **14**, 1943 (1984); H. Yamada, Physica B+C **149B**, 390 (1988), and references therein.
- ⁶K. Schwarz and P. Mohn, J. Phys. F **74**, L129 (1984).
- ⁷P. Mohn and K. Schwarz, Physica B+C **130B**, 26 (1985).
- ⁸M. Sagawa, S. Fujimura, N. Togawa, H. Yamamoto, and Y. Matsuura, J. Appl. Phys. **55**, 2083 (1984).
- ⁹J. J. Croat, J. F. Herbst, R. W. Lee, and F. E. Pinkerton, Appl. Phys. Lett. **44**, 148 (1984).
- ¹⁰D. B. de Mooij and K. H. J. Buschow, J. Less-Common Met. **136**, 207 (1988); and unpublished.
- ¹¹K. Ohashi, T. Yokoyama, R. Osugi, and Y. Tawara, IEEE Trans. Magn. **MAG-23**, 3101 (1987); K. Ohashi, Y. Tawara, R. Osugi, J. Sakurai, and Y. Komura, J. Less-Common Met. **139**, L1 (1988).
- ¹²R. Coehoorn (unpublished).
- ¹³J. Le Roy, J. M. Moreau, C. Bertrand, and M. A. Fremy, J. Less-Common Met. **136**, 19 (1987).
- ¹⁴D. B. de Mooij and K. H. J. Buschow (private communication).
- ¹⁵A. Kostikas and D. Niarchos (unpublished).
- ¹⁶F. J. Cadieu, T. D. Cheung, S. H. Aly, L. Wickramasekara, and R. G. Pirich, J. Appl. Phys. **53**, 8338 (1982); F. J. Cadieu, T. D. Cheung, L. Wickramasekara, and S. H. Aly, *ibid.* **55**, 2611 (1984).
- ¹⁷S. M. Kanetkar, G. C. Hadjipanayis, A. Nazareth, and S. C. Cheng, in *Proceedings of the International Symposium of Physics of Materials, Sendai (Japan)*, edited by M. Takahashi, S. Maekawa, Y. Gondo, and H. Nosé (World Scientific, Singapore, 1987), p. 391.
- ¹⁸E. Parthé and R. Lemaire, Acta Crystallogr. Sect. B **31**, 1879 (1975).
- ¹⁹K. H. J. Buschow, J. Less-Common Met. **11**, 204 (1966).
- ²⁰P. C. M. Gubbens, J. J. v. Loef, and K. H. J. Buschow, J. Phys. (Paris) Colloq. (Suppl. 12) **35**, C6-617 (1974).
- ²¹A. R. Williams, J. Kübler, and C. D. Gelatt, Jr., Phys. Rev. B **19**, 6094 (1979).
- ²²U. von Barth and L. Hedin, J. Phys. C **5**, 1629 (1972).
- ²³J. F. Janak, Solid State Commun. **25**, 53 (1978).
- ²⁴M. Weinert, E. Wimmer, and A. J. Freeman, Phys. Rev. B **24**, 864 (1981).
- ²⁵E. P. Wohlfahrt, *Ferromagnetic Materials* (North-Holland, Amsterdam, 1980), Vol. 1.
- ²⁶S. Sinnema, Ph.D. thesis, University of Amsterdam, 1988.
- ²⁷D. Givord, F. Givord, and R. Lemaire, J. Phys. (Paris) Colloq. (Suppl. 2-3) **32**, C1-668 (1971).
- ²⁸C. A. Beckman, K. S. V. L. Narasimhan, W. E. Wallace, R. S. Craig, and R. A. Butera, J. Phys. Chem. Solids **37**, 245 (1976).
- ²⁹H. R. Kirchmayr and W. Steiner, J. Phys. (Paris) Colloq. **32**, C1-665 (1971).
- ³⁰J. F. Herbst and J. J. Croat, J. Appl. Phys. **53**, 4304 (1982).
- ³¹K. H. J. Buschow and R. P. van Staple, J. Phys. (Paris) Colloq. **32**, C1-672 (1971).
- ³²R. A. Reck and D. L. Fry, Phys. Rev. **184**, 492 (1969).
- ³³B. Szpunar, J. Less-Common Met. **127**, 55 (1987).
- ³⁴P. C. M. Gubbens, J. H. F. van Apeldoorn, A. M. van der Kraan, and K. H. J. Buschow, J. Phys. F **4**, 921 (1974).
- ³⁵A. M. van der Kraan, P. C. M. Gubbens, and K. H. J. Buschow, Phys. Status Solidi A **31**, 495 (1975).
- ³⁶J. Rhyne, J. Magn. Magn. Mater. **70**, 88 (1987).
- ³⁷A. Oppelt and K. H. J. Buschow, J. Phys. F **3**, L212 (1973).
- ³⁸T. Dumelow, P. C. Riedi, P. Mohn, K. Schwarz, and Y. Yamada, J. Magn. Magn. Mater. **54-57**, 1081 (1986).
- ³⁹V. L. Moruzzi, J. F. Janak, and A. R. Williams, *Calculated Electronic Properties of Metals* (Pergamon, New York, 1978).
- ⁴⁰G. H. O. Daalderop and H. J. F. Jansen (private communication).
- ⁴¹K. B. Hathaway, H. J. F. Jansen, and A. J. Freeman, Phys. Rev. B **31**, 7603 (1985).
- ⁴²S. H. Vosko, L. Wilk, and M. Nusair, Can. J. Phys. **58**, 1200 (1980).
- ⁴³C. S. Wang, B. M. Klein, and H. Krakauer, Phys. Rev. Lett. **54**, 1852 (1985).
- ⁴⁴H. J. F. Jansen and S. S. Peng, Phys. Rev. B **37**, 2689 (1988).
- ⁴⁵A. M. Olés and G. Stollhoff, J. Magn. Magn. Mater. **54-57**, 1045 (1986).
- ⁴⁶P. R. Subramanian and J. F. Smith, CALPHAD **8**, 295 (1984).
- ⁴⁷J. Mathon, J. Phys. F **2**, 159 (1972).
- ⁴⁸V. L. Moruzzi, P. M. Marcus, K. Schwarz, and P. Mohn, Phys. Rev. B **34**, 1784 (1986).
- ⁴⁹M. Shimizu, Rep. Prog. Phys. **44**, 309 (1981).
- ⁵⁰J. G. M. Armitage, T. Dumelow, R. H. Mitchell, P. C. Riedi, J. S. Abell, P. Mohn, and K. Schwarz, J. Phys. F **16**, L141 (1986).